

Novel CD8⁺ T Cell Antagonists Based on β_2 -Microglobulin*

Received for publication, February 22, 2002
Published, JBC Papers in Press, March 25, 2002, DOI 10.1074/jbc.M201819200

Meir Glick‡, David A. Price§¶, Anne-Lise Vuidepot||, Torben B. Andersen||, Sarah L. Hutchinson§, Bruno Laugel§, Andrew K. Sewell§, Jonathan M. Boulter||, P. Rod Dunbar§, Vincenzo Cerundolo§, Annette Oxenius§, John I. Bell§, W. Graham Richards‡, and Bent K. Jakobsen||**

From the ‡Department of Chemistry, Central Chemistry Laboratory, University of Oxford, South Parks Road, Oxford OX1 3QH, the §Nuffield Department of Clinical Medicine, Level 7, John Radcliffe Hospital, Headington, Oxford OX3 9DU, and ||Avidex Ltd., 57 Milton Park, Abingdon, Oxon OX14 4RX, United Kingdom

The CD8 coreceptor of cytotoxic T lymphocytes binds to a conserved region of major histocompatibility complex class I molecules during recognition of peptide-major histocompatibility complex (MHC) class I antigens on the surface of target cells. This event is central to the activation of cytotoxic T lymphocyte (CTL) effector functions. The contribution of the MHC complex class I light chain, β_2 -microglobulin, to CD8 $\alpha\alpha$ binding is relatively small and is mediated mainly through the lysine residue at position 58. Despite this, using molecular modeling, we predict that its mutation should have a dramatic effect on CD8 $\alpha\alpha$ binding. The predictions are confirmed using surface plasmon resonance binding studies and human CTL activation assays. Surprisingly, the charge-reversing mutation, Lys⁵⁸ → Glu, enhances β_2 m-MHC class I heavy chain interactions. This mutation also significantly reduces CD8 $\alpha\alpha$ binding and is a potent antagonist of CTL activation. These results suggest a novel approach to CTL-specific therapeutic immunosuppression.

The peptide-MHC¹ class I complex (pMHC) on a target cell (antigen presenting cell) is recognized by a specific T cell receptor on the surface of CD8⁺ cytotoxic T lymphocytes (CTL). The pMHC consists of a heavy chain, which is attached to the cell membrane and contains the peptide binding site, and a light chain, β_2 -microglobulin (β_2 m). The CD8 molecule is a cell-surface glycoprotein present on CTL, which acts as a “co-receptor”; it is not peptide-specific, but binds to a conserved site on the pMHC molecule, which comprises several regions on the heavy chain and the small DE loop of β_2 m consisting of residues 58–60 (Lys⁵⁸-Asp⁵⁹-Trp⁶⁰) (1).

After CTL engage pMHC, the earliest intracellular events

induce specific phosphorylation of tyrosine residues in the immunoreceptor tyrosine activation motifs within the cytoplasmic tails of the TCR-associated CD3 complex. The cytoplasmic tail of the CD8 α -chain is associated with the protein tyrosine kinase p56^{lck}. Active p56^{lck} initiates TCR signal transduction by phosphorylating the immunoreceptor tyrosine activation motifs within the CD3 complex. Inhibition of CD8 binding to pMHC therefore inhibits T cell activation (2).

Exogenous soluble β_2 m can exchange with cell surface-associated β_2 m complexed to pMHC (3). Therefore, by mutating the CD8 contact site on β_2 m, and exchanging the mutant β_2 m into the native MHC, it should be possible to inhibit CTL activation.

EXPERIMENTAL PROCEDURES

Molecular Dynamics and Free Energy Perturbations—Initial coordinates were taken from the crystal structure of the complex between human MHC class I HLA-A2 and the T cell coreceptor CD8 $\alpha\alpha$ solved at 2.65-Å resolution and deposited in the Protein Data Bank (4) under the name 1akj (1). Molecular dynamics and free energy perturbations were performed using CHARMM (version 27) (5) and the standard all-atom parameter set (6). Hydrogens were added using the HBUILD module in CHARMM. Water molecules were added to the complex by superimposing a 16-Å sphere of TIP3P water molecules centered at the β_2 m Lys⁵⁸ N ζ atom.

The solvent atoms were minimized by 500 steps of steepest descents followed by 1000 steps of conjugate gradient. At the next step, the entire system was relaxed with 500 steps of steepest descents that were switched to conjugate gradient until convergence criteria of r.m.s. gradient of the potential energy lower than 0.3 Kcal/mol·Å has been achieved. A 14-Å nonbonded cutoff was employed. The dielectric constant was unity. The system was simulated using a stochastic boundary molecular dynamics (7). The reference point for partitioning the system was the β_2 m Lys⁵⁸ N ζ atom. The system was divided into a 12-Å reaction region, a 4-Å buffer region, and a reservoir. The frictional coefficients for water oxygen and heavy atoms in the protein were 62 and 200 ps⁻¹, respectively (8). The relaxed system was equilibrated at 300 K for 150 ps with a time step of 1 fs followed by 1 ns performed for data collection with coordinates and energies saved to a disc every 1 ps. The β_2 m Lys⁵⁸ was mutated using the Biopolymer and Homology modules in the MSI software package. For each mutation the procedure described above has been repeated. Relative binding Helmholtz free energies were calculated by the perturbation method (9) as follows: $\Delta G_3 = \text{HLA-A2}/\beta_2\text{m}_{(\text{native})} \text{ complex} \rightarrow \text{HLA-A2}/\beta_2\text{m}_{(\text{Lys} \rightarrow \text{Glu})} \text{ complex}$ and $\Delta G_4 = \text{HLA-A2}/\beta_2\text{m}_{(\text{native})}/\text{CD8}\alpha\alpha \text{ complex} \rightarrow \text{HLA-A2}/\beta_2\text{m}_{(\text{Lys} \rightarrow \text{Glu})}/\text{CD8}\alpha\alpha \text{ complex}$.

Since free energy is a state function, it is path-independent, and the free energy difference: $\Delta G_4 - \Delta G_3$ is equal to the difference $\Delta G_2 - \Delta G_1$ (see “Results”). Each perturbation was performed in two steps using a total number of 26 windows. At the first 16 windows the lysine H δ 1, H ϵ 1, H ϵ 2, N ζ , H ζ 1, H ζ 2, and H ζ 3 atoms (including their charges) were deleted. C δ atom type was modified to sp² carbonyl carbon. H δ 2 and C ϵ atom types were modified to carboxylate oxygens. At the last 10 windows, the charges of the remaining side chain were adjusted to asp side chain. Trajectories were produced by MD simulations at the same conditions to these described above with 150 ps of equilibration and 100 ps of data collection at every window.

Soluble CD8 $\alpha\alpha$ Preparation—The extracellular fragment of soluble CD8 $\alpha\alpha$ (residues 1–120) was expressed in *Escherichia coli*, refolded and

* This work was supported by the Medical Research Council (to D. A. P. and J. I. B.), the Wellcome Trust (to A. K. S., B. L., M. G., and S. L. H.), EMBO (to A. O.), and Avidex Ltd. (to A.-L. V., B. K. J., J. M. B., and T. B. A.). The costs of publication of this article were defrayed in part by the payment of page charges. This article must therefore be hereby marked “advertisement” in accordance with 18 U.S.C. Section 1734 solely to indicate this fact.

¶ Medical Research Council Clinician Scientist.

** To whom correspondence should be addressed: Avidex Ltd., 57 Milton Park, Abingdon, Oxon OX14 4RX, UK. Tel.: 44-1235-438603; Fax: 44-1235-438601; E-mail: bent.jakobsen@avidex.com.

¹ The abbreviations used are: MHC, major histocompatibility complex; pMHC, peptide-MHC class I complex; CTL, cytotoxic T lymphocyte(s); β_2 m, β_2 -microglobulin; TCR, T cell receptor; r.m.s., root mean square; MD, molecular dynamic; B-LCL, B-lymphoblastoid cell line(s); rVV, recombinant vaccinia virus; RANTES, regulated on activation normal T cell expressed and secreted; SPR, surface plasmon resonance; PBMC, peripheral blood mononuclear cell(s); HIV-1, human immunodeficiency virus, type 1.

TABLE I
Molecular dynamics results for the interaction between the CD8 $\alpha\alpha$ and β_2 m Lys⁵⁸/mutants

Hydrogen bonds to the CD8 $\alpha\alpha$ ^a					
System	Donor	H	Acceptor	Distance D . . A	Angle D, . . H . . A
Crystal structure	Lys ⁵⁸ N ζ (β_2 m)		Asp ⁷⁵ O δ 2 (CD8 α -1)	2.68	
	Lys ⁵⁸ N ζ (β_2 m)		Val ²⁴ O (CD8 α -1)	2.98	
MD native structure	Lys ⁵⁸ N ζ (β_2 m)	Lys ⁵⁸ H ζ 3 (β_2 m)	Asp ⁷⁵ O δ 2 (CD8 α -1)	2.60	167.3
	Lys ⁵⁸ N ζ (β_2 m)	Lys ⁵⁸ H ζ 2 (β_2 m)	Val ²⁴ O (CD8 α -1)	2.71	164.3
MD Lys ⁵⁸ \rightarrow Arg	Lys ⁵⁸ N η 1 (β_2 m)	Arg ⁵⁸ H η 11 (β_2 m)	Asp ⁷⁵ O δ 2 (CD8 α -1)	2.65	154.9
MD Lys ⁵⁸ \rightarrow Ser	Ser ⁵⁸ O γ (β_2 m)	Ser ⁵⁸ H γ (β_2 m)	H ₂ O 45 O	2.68	168.3
	H ₂ O 45 O	H ₂ O 45 H ₁	Val ²⁴ O (CD8 α -1)	2.66	140.0
MD Lys \rightarrow Cys	Cys ⁵⁸ S γ (β_2 m)	Cys ⁵⁸ H γ (β_2 m)	H ₂ O 60 I	4.32 ^b	97.0 ^b
	H ₂ O 60 O	H ₂ O 60 H ₂	Val ²⁴ O (CD8 α -1)	2.69	160.5
Time averaged r.m.s. deviation of contact residues to the crystal structure ^c					
β_2 m Lys ⁵⁸ mutation				Contact residues r.m.s.	
MD native structure					
Lys ⁵⁸ \rightarrow Arg				0.65	
Lys ⁵⁸ \rightarrow Ser				0.66	
Lys \rightarrow Glu				0.70	
Lys ⁵⁸ \rightarrow Lys ⁵⁸ neutral				0.71	
Lys ⁵⁸ \rightarrow Asp				0.75	
Lys ⁵⁸ \rightarrow Tyr				0.87	
Lys ⁵⁸ \rightarrow Cys				0.91	
Lys ⁵⁸ \rightarrow Trp				0.93	
Lys ⁵⁸ \rightarrow Val				0.94	
Lys ⁵⁸ \rightarrow GRG ^d				1.00	
Lys ⁵⁸ \rightarrow SES				1.21	
				1.78	

^a Time averaged distance between donor D and acceptor A is less than 3.2 Å (except a sulfur donor, where the distance between donor and acceptor is less than 3.6 Å). D-H . . A angle between 140° and 180°. Lys⁵⁸ \rightarrow Lys⁵⁸ neutral, Lys⁵⁸ \rightarrow Glu, Lys⁵⁸ \rightarrow Tyr, Lys⁵⁸ \rightarrow Trp, Lys⁵⁸ \rightarrow GRG and Lys⁵⁸ \rightarrow SES mutants did not form any H-bonds with Asp⁷⁵ O δ 2 or Val²⁴ O.

^b Although the average bond length is larger than 3.6 Å, 85 frames show hydrogen bonds that obey the above criteria.

^c r.m.s. values given in Å. Comparison included all contact residues non hydrogen atoms according to Gao *et al.* (1) (total number of 61 atoms) CD8 α -1: Arg⁴, Asp⁷⁵, Val²⁴-Val²⁶, β_2 m: Trp⁶⁰, Lys⁵⁸ (mutated) where only the backbone and C β are included in residue 58 since side chain is mutated.

^d Only 60 atoms were included in comparison, since glycine does not contain a C β atom.

purified as described previously (1). The CD8 $\alpha\alpha$ concentration was determined from the extinction coefficient (32,480 M⁻¹ × cm⁻¹, determined by amino acid analysis), assuming 100% activity.

Soluble TCR Preparation—The TCR used for the SPR experiments derives from the JM22 T cell clone (10, 11). It is specific for an HLA-A2-restricted peptide (GILGFVFTL) from the influenza matrix protein (58–66) and uses gene segments TCRAV10S2J9S11C1 and TCRBV17S1J2S7C2. The two fragments of soluble JM22-TCR $\alpha\beta$ (residues 1–204 for the α -chain and 1–245 for the β -chain) were expressed in *E. coli*, refolded and purified as described previously (12). The TCR concentration was determined from the extinction coefficient (105,500 M⁻¹ × cm⁻¹, determined by amino acid analysis), assuming 100% activity.

Soluble HLA-A2/ β_2 m Complex Preparation—Soluble influenza peptide-HLA-A2/ β_2 m complexes were prepared by refolding HLA-A2 heavy chain carrying the biotin tag with β_2 m wildtype or mutant (both expressed in *E. coli*) and the synthetic peptide corresponding to influenza matrix protein 58–66 GILGFVFTL (Genosys, Woodlands, TX) as described in Garboczi *et al.* (13). The refolded complexes were purified by both anion exchange and gel filtration before being used in SPR experiments. HLA-A2 heavy chain was enzymatically biotinylated as described (14) using *N*-hydroxysuccinimidobiotin (Sigma) and BirA enzyme. Tetrameric pMHC I complexes were produced by conjugation with phycoerythrin-labeled extravidin as described previously (14). DNA constructs encoding the β_2 m mutants (Lys⁵⁸ to Arg, Asp, Glu, Ser, Val, Tyr, Cys, SES, Trp, and GRG) were produced using the Quick-Change Site-Directed Mutagenesis Kit (Stratagene) and checked by DNA sequencing of the entire coding fragment. The mutant proteins were expressed and the inclusion bodies purified as for the wild type.

Surface Plasmon Resonance Experiments—SPR binding studies were performed at 25 °C using a BIAcoreTM 3000 (BIAcore AB, St. Albans, UK) in HBS (BIAcore AB). HBS contains 10 mM HEPES, pH 7.4, 150 mM NaCl, 3.4 mM EDTA, and 0.005% Surfactant P20. Peptide-HLA class I complex was bound to the BIAcore chip by producing recombinant soluble pMHC fused to a biotinylation tag, which was specifically biotinylated *in vitro* (14) and flowed over a streptavidin-coated chip surface. Streptavidin (Sigma) was covalently coupled to Research Grade CM5 sensor chip (BIAcore) via primary amines using the Amine Coupling kit (BIAcore). For coupling, the streptavidin was dissolved in 10 mM sodium acetate, pH 5.5, and injected at 0.2 mg ml⁻¹. Immobilization level

was 6000 response units on average. Biotinylated HLA-A2/ β_2 m (wild type and mutants) complexes were immobilized at 12,000–12,500 Response units by injection of 5–35 μ l at 40–100 μ g ml⁻¹, at a flow rate of 5 μ l min⁻¹. The injections of the different CD8 $\alpha\alpha$ (sCD8) and JM22-TCR $\alpha\beta$ (sTCR) solutions were performed at a flow rate of 5 μ l min⁻¹. K_d values were obtained either by Scatchard plots or by nonlinear fitting of the Langmuir binding isotherm ($A + B \leftrightarrow AB$) equation [$AB = B \times AB_{\max}/(K_d + B)$] (where B is sCD8 (or sTCR) concentration and AB_{\max} is maximum sCD8 (or sTCR) binding) to the data using the Levenberg-Marquardt algorithm as implemented in the Windows 98 application Origin (version 6.1; Microcal Software, Northampton, MA).

Cell Culture and CTL Activation Assays—pBMC were isolated from fresh blood by Ficoll-Hypaque density gradient centrifugation. CD8⁺ CTL clones were generated and maintained as described previously (15). Target cells in cytotoxicity assays were HLA-matched immortalized T cell hybridomas or Epstein-Barr virus transformed B-lymphoblastoid cell lines (B-LCL) incubated with peptide as shown, or infected with recombinant vaccinia virus (rVV), and labeled with ⁵¹Cr (Amersham Biosciences, Amersham, UK). Peptides were synthesized using standard Fmoc (*N*-(9-fluorenyl)methoxycarbonyl) chemistry and were >90% pure as determined by high performance liquid chromatography (Research Genetics, Huntsville, AL). Vaccinia infections were effected at 3–5 plaque-forming units/cell for 1 h and followed by a 6-h incubation period to allow expression prior to ⁵¹Cr labeling. The rVV expressing HIV-1 Nef was constructed from a full-length proviral clone isolated from donor SC1 according to standard protocols; wild type WR rVV was used to infect control target cells (16). Lysis assays were performed in low percentage fetal calf or human serum using standard ⁵¹Cr release methodology (17). Tetrameric pMHC I complex activation assays were performed by measurement of extracellular RANTES release after 30-min exposure as described previously (18). All data points for both lysis and RANTES release assays represent the mean of triplicate readings; *y* axis error bars show the S.D. in each case.

Flow Cytometric Analysis—Cells were stained with phycoerythrin-labeled tetrameric pMHC I complexes containing wildtype or Lys⁵⁸ \rightarrow Glu forms of β_2 m as described previously (19). Stained cells were analyzed using a Becton Dickinson Calibur flow cytometer with CellQuest software.

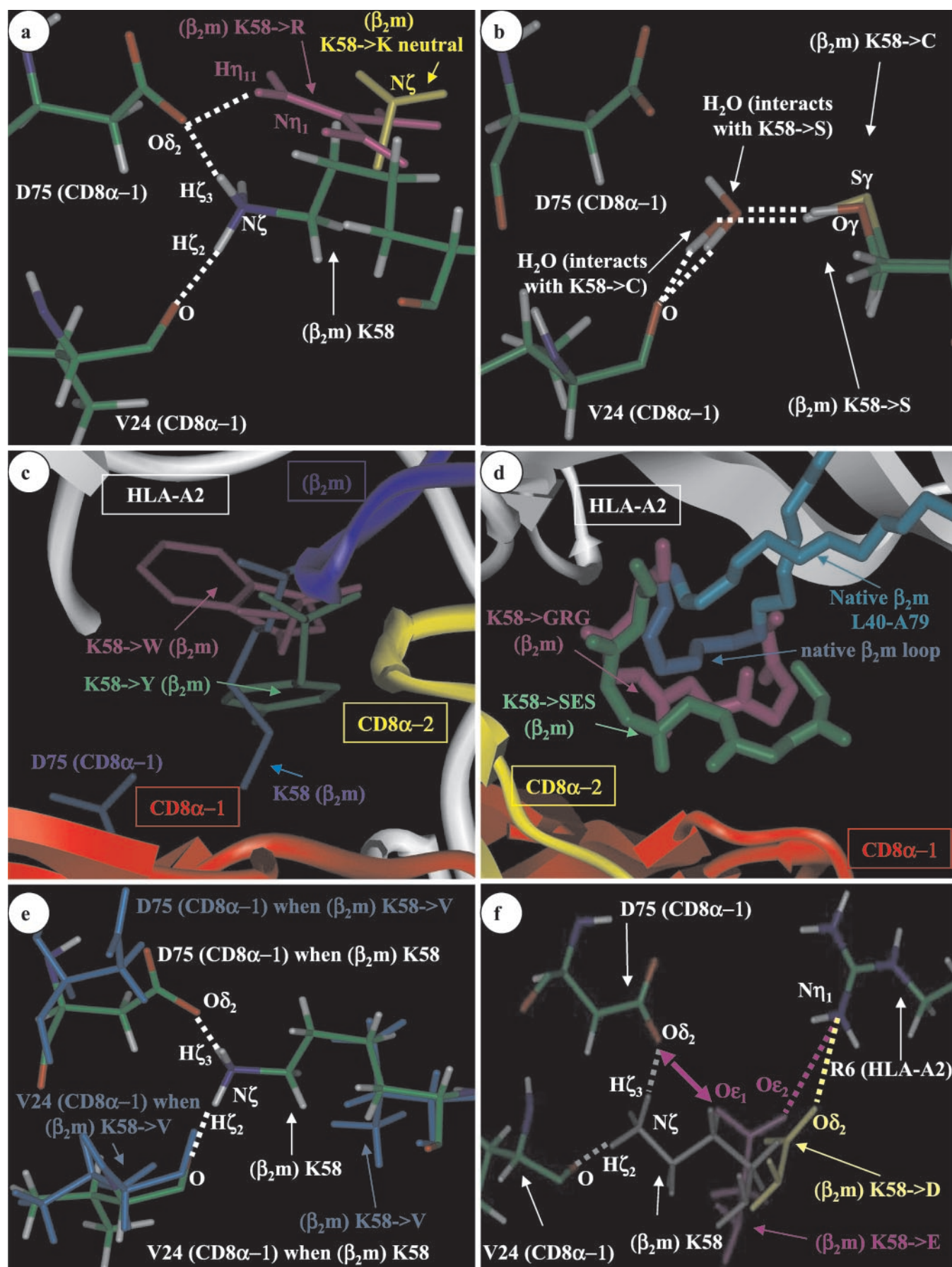


FIG. 1. The effect of various β_2 m Lys⁵⁸ mutations on the interaction with the CD8 α and HLA-A2 molecules. H-bonds are shown in hashed lines, atom colors: carbon (C) = green; nitrogen (N) = blue; oxygen (O) = red; hydrogen (H) = white; sulfur (S) = yellow. a, the importance of the positive charge on Lys⁵⁸ side chain. While the native Lys⁵⁸ forms two H-bonds to CD8 α -1 Asp⁷⁵ and Val²⁴, neutral lysine (side chain in yellow)

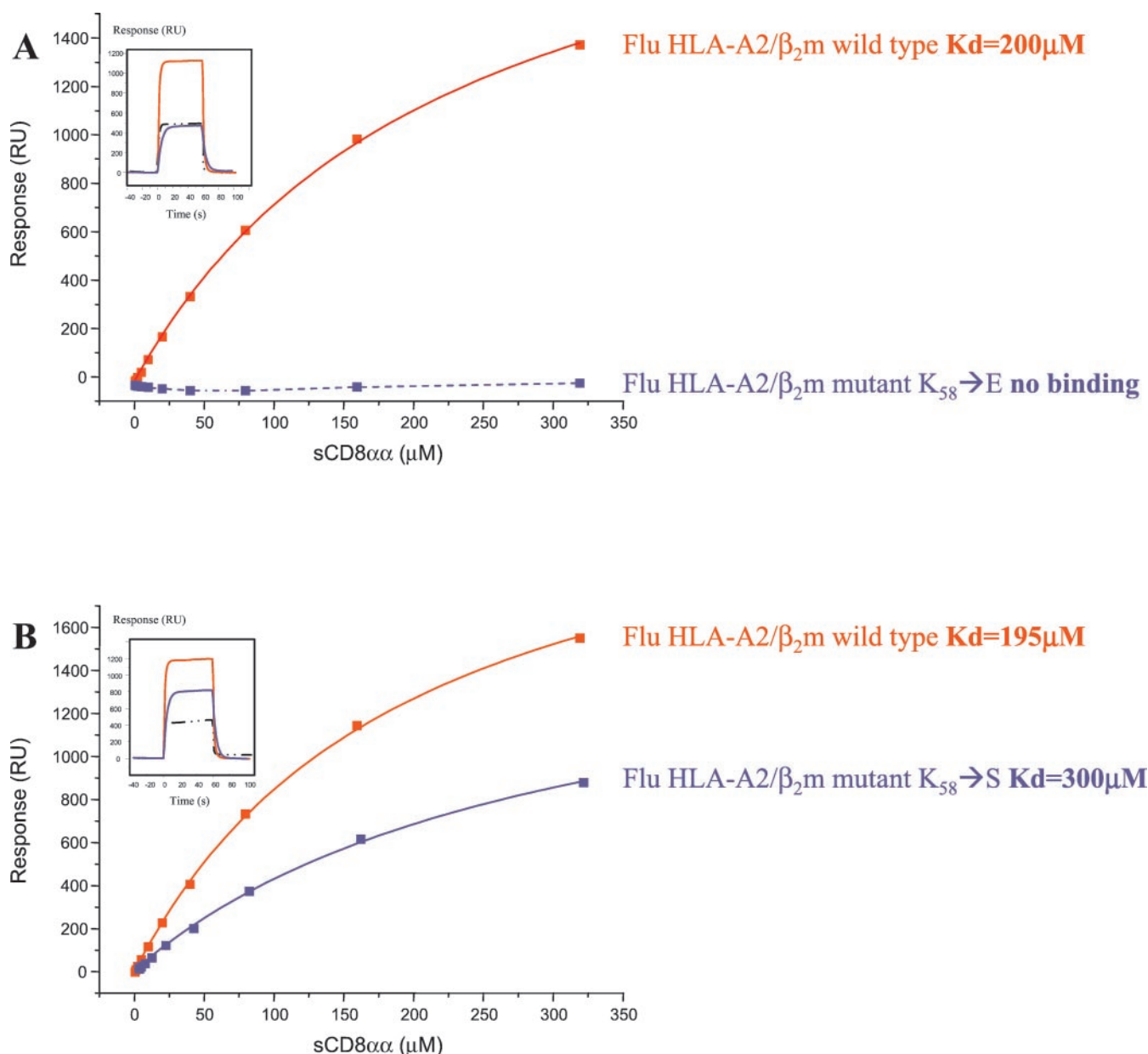


FIG. 2. The affinity of CD8 $\alpha\alpha$ binding to HLA-A2/ β_2 m complexes. *a*, CD8 $\alpha\alpha$ was injected at increasing concentrations for 1 min through flow cells where HLA-A2/ β_2 m wild type (positive control), HLA-A2/ β_2 m mutant Lys⁵⁸ \rightarrow Glu were coupled via biotinylated heavy chain and through a flow cell with no protein immobilized (negative control). The amount of CD8 $\alpha\alpha$ that bound to the HLA-A2/ β_2 m complexes at each concentration was calculated as the difference between the responses at equilibrium in the HLA-A2/ β_2 m complexes and the negative control flow cells and is plotted against the CD8 $\alpha\alpha$ concentration. *b*, a similar experiment was performed with the HLA-A2/ β_2 m mutant Lys⁵⁸ \rightarrow Ser complex. In *a* and *b*, the *solid lines* represent nonlinear fits of the Langmuir binding to the data. In *a*, the responses obtained for the HLA-A2/ β_2 m mutant Lys⁵⁸ \rightarrow Glu were too low, and it was not possible to fit the data (*blue dotted line*). These experiments were performed at $5\ \mu\text{l}\ \text{min}^{-1}$. *Insets*, responses obtained in the blank cell (*black dotted line*), in the HLA-A2/ β_2 m wild type cell (*red line*), and in the HLA-A2/ β_2 m Lys⁵⁸ \rightarrow Glu for *a* and Lys⁵⁸ \rightarrow Ser for *b* cell (*blue line*) during the CD8 $\alpha\alpha$ ($80\ \mu\text{M}$) injection.

RESULTS AND DISCUSSION

We employed 1-ns MD simulations to study the interactions between CD8 $\alpha\alpha$, HLA-A2, and β_2 m molecules. We focused on the β_2 m Lys⁵⁸ residue, which forms two key hydrogen bonds

with CD8 α -1 Asp⁷⁵ O δ 2 and Val²⁴ O (1), to design and predict the effects of novel β_2 m mutants on the interaction between CD8 $\alpha\alpha$ and pMHC. Five classes of Lys⁵⁸ mutations were studied: a mutation that preserves the positive charge (Lys⁵⁸ \rightarrow Arg),

does not interact with the CD8 α -1. In the Lys⁵⁸ \rightarrow Arg mutant (side chain in *purple*) the H-bond to CD8 α -1 Asp⁷⁵ is preserved. *b*, in the Lys⁵⁸ \rightarrow Ser and Lys⁵⁸ \rightarrow Cys mutants the interaction with the CD8 $\alpha\alpha$ is mediated through a water molecule: the side chain donates its hydroxyl or thiol hydrogen to a water molecule, which donates its hydrogen to CD8 $\alpha\alpha$ Val²⁴ carbonyl oxygen. *c*, the native structure β_2 m Lys⁵⁸ and CD8 α -1 Asp⁷⁵ (*blue*) compared with steric hindrance via a bulky side chain mutants: Lys⁵⁸ \rightarrow Tyr (side chain in *green*) and Lys⁵⁸ \rightarrow Trp (side chain in *purple*). The bulky side chain fills the cavity between the HLA-A2/ β_2 m CD8 $\alpha\alpha$, and the interaction with the CD8 $\alpha\alpha$ is poor. *d*, comparison between the native β_2 m DE loop consisting of residues 58–60 (Lys⁵⁸-Asp⁵⁹-Trp⁶⁰), shown in *blue*, to insertions: Lys⁵⁸ \rightarrow SES (*green*) and Lys⁵⁸ \rightarrow GRG (*purple*). β_2 m residues Leu⁴⁰-Ala⁷⁹ are shown in *azure*. *e*, comparison between the native structure to a Lys⁵⁸ \rightarrow Val mutation (*blue*). The hydrophobic valine side chain repels CD8 α -1 Asp⁷⁵ carboxylate. *f*, mutations to a negatively charged side chain: Lys⁵⁸ \rightarrow Asp (*yellow*), Lys⁵⁸ \rightarrow Glu (*purple*) compared with the native lysine (*gray*). In both Lys⁵⁸ \rightarrow Asp and Lys⁵⁸ \rightarrow Glu mutations the positive charge on HLA-A2 Arg⁶ heavy chain attracts the mutant's carboxylate. Only Lys⁵⁸ \rightarrow Glu carboxylate is in close proximity to CD8 α -1 Asp⁷⁵ O δ 2.

TABLE II
 Summary of affinity constants

Immobilized complex	Soluble CD8 α binding (K_d in μM) ^a	Soluble JM22-TCR $\alpha\beta$ binding (K_d in μM) ^a
Flu-HLA-A2/ β_2 m wild type	165 \pm 35 ($n = 9$)	8.6 \pm 2 ($n = 7$)
Flu-HLA-A2/ β_2 m mutant Lys ⁵⁸ \rightarrow Arg	300 ($n = 1$) ^b	10.6 ($n = 1$)
Flu-HLA-A2/ β_2 m mutant Lys ⁵⁸ \rightarrow Ser	301 \pm 1 ($n = 2$)	10.5 ($n = 1$)
Flu-HLA-A2/ β_2 m mutant Lys ⁵⁸ \rightarrow Cys	558 ($n = 1$) ^b	10.4 ($n = 1$)
Flu-HLA-A2/ β_2 m mutant Lys ⁵⁸ \rightarrow Val	1084 ($n = 1$)	7.1 ($n = 1$)
Flu-HLA-A2/ β_2 m mutant Lys ⁵⁸ \rightarrow Glu	NB ($n = 4$) ^c	8.8 \pm 0.8 ($n = 4$)
Flu-HLA-A2/ β_2 m mutant Lys ⁵⁸ \rightarrow Asp	NB ($n = 1$) ^c	7.9 ($n = 1$)
Flu-HLA-A2/ β_2 m mutant Lys ⁵⁸ \rightarrow Tyr	NB ($n = 2$) ^{b,c}	8.6 \pm 1 ($n = 2$)
Flu-HLA-A2/ β_2 m mutant Lys ⁵⁸ \rightarrow Trp	NB ($n = 1$) ^c	4.9 ($n = 1$)
Flu-HLA-A2/ β_2 m mutant Lys ⁵⁸ \rightarrow SES	NB ($n = 1$) ^{b,c}	8.5 ($n = 1$)
Flu-HLA-A2/ β_2 m mutant Lys ⁵⁸ \rightarrow GRG	NB ($n = 1$) ^c	6.2 ($n = 1$)

^a Mean \pm deviation from n independent determinations at 25 °C.

^b Similar results were obtained with another peptide.

^c No binding (response too low to determine a K_d).

mutations to short polar side chains (Lys⁵⁸ \rightarrow Ser, Lys⁵⁸ \rightarrow C), mutations introducing steric hindrances via bulky side chains (Lys⁵⁸ \rightarrow Tyr, Lys⁵⁸ \rightarrow Trp) or insertions (Lys⁵⁸ \rightarrow SES, Lys⁵⁸ \rightarrow GRG), a mutation to a medium length hydrophobic side chain (Lys⁵⁸ \rightarrow Val), mutations to negatively charged side chains (Lys⁵⁸ \rightarrow Asp, Lys⁵⁸ \rightarrow Glu).

We studied the hydrogen bond network formed between the wild type Lys⁵⁸, or mutations of this residue, to CD8 α -1 as shown in Table I. The perturbation to the conformation of the contact residues (CD8 α -1:Arg⁴, Asp⁷⁵, Val²⁴-Val²⁶, β_2 m:Trp⁶⁰, Lys⁵⁸) (1) caused by various Lys⁵⁸ mutations is presented as the root mean square (r.m.s.) deviation of these residues to that observed in the crystal structure.

Neutralizing the Lys⁵⁸ positive charge *in silico* leads to the loss of two H-bonds to CD8 α -1 Asp⁷⁵ O δ 2 and Val²⁴ O atoms, as illustrated in Fig 1a and Table I, and formation of alternative hydrogen bonds with water molecules in the cavity of the HLA-A2/CD8 α / β_2 m complex. A mutation that preserves the positive charge (Lys⁵⁸ \rightarrow Arg) has a less dramatic effect: the H-bond to CD8 α -1 Asp⁷⁵ O δ 2 is preserved, and the r.m.s. value is similar to that of the wild type structure and smaller than that of the neutral Lys⁵⁸ side chain. Therefore, eliminating the positive charge on the side chain is likely to reduce the binding affinity to the CD8 α .

In short polar side chain mutants, Lys⁵⁸ \rightarrow Ser and Lys⁵⁸ \rightarrow Cys, the interaction with CD8 α is mediated through a water molecule as shown in Fig. 1b and Table I. The side chain donates its hydroxyl or thiol hydrogen to a water molecule, which donates its hydrogen to CD8 α Val²⁴ O. Unlike Lys⁵⁸ \rightarrow Ser, where the H-bond network is stable, the H-bond between the thiol moiety and the water molecule in the Lys⁵⁸ \rightarrow Cys mutant fluctuates during the simulation. This has an impact on the r.m.s. values shown in Table I, which increase from 0.70 for Lys⁵⁸ \rightarrow Ser to 0.93 for Lys⁵⁸ \rightarrow Cys. These results suggest that removing the H-donor group from the side chain at position 58 should reduce the binding affinity to CD8 α .

Mutations introducing steric hindrance via a bulky side chain, Lys⁵⁸ \rightarrow Tyr and Lys⁵⁸ \rightarrow Trp, are illustrated in Fig. 1c. The bulky side chain fills the cavity between HLA-A2/ β_2 m and CD8 α , and the interaction with CD8 α is impaired by the lack of H-bonding, resulting in high r.m.s. values (Table I). Lys⁵⁸ \rightarrow GRG and Lys⁵⁸ \rightarrow SES insertions (Fig. 1d) perturb the tertiary structure and lead to increased r.m.s. values of 1.21 and 1.78, respectively. The higher r.m.s. value of the Lys⁵⁸ \rightarrow SES insertion is due to reversal of the positive charge and the fact that serine has a side chain that contributes to the overall steric hindrance.

The Lys⁵⁸ \rightarrow Val mutation yielded a higher r.m.s. value than all other single substitution mutations. In bulkier mutations,

such as Lys⁵⁸ \rightarrow Trp, the side chain can orient itself toward the HLA-A2/ β_2 m-CD8 α cavity, whereas the valine side chain is not long enough to have this effect. As a result, the hydrophobic side chain repels the polar CD8 α -1 Asp⁷⁵ (Fig. 1e).

Fig. 1f shows mutations to a negatively charged side chain (Lys⁵⁸ \rightarrow Asp, Lys⁵⁸ \rightarrow Glu). Repulsion between the carboxylates leads to an average distance of 6.27 Å between the CD8 α -1 Asp⁷⁵ O δ 2 and Lys⁵⁸ \rightarrow Asp O δ 1 oxygens. Strikingly, the distance between CD8 α -1 Asp⁷⁵ O δ 2 and Glu⁵⁸ O ϵ 1 oxygens in the Lys⁵⁸ \rightarrow Glu is only 4.09 Å. Both Lys⁵⁸ \rightarrow Asp and Lys⁵⁸ \rightarrow Glu are attracted to the positive charge on HLA-A2 Arg⁶ heavy chain: in 52.9% of the frames taken from the MD simulation, the distance between the mutated Glu⁵⁸ O ϵ 2 and HLA-A2 Arg⁶ N η 1 atoms was lower than 5 Å, fluctuating to a minimum of 3.18 Å. This interaction stabilizes the HLA-A2/ β_2 m complex and orients the Lys⁵⁸ \rightarrow Glu side chain toward CD8 α -1 Asp⁷⁵. HLA-A2 Arg⁶ heavy chain attracts the Lys⁵⁸ \rightarrow Asp carboxylate as well; however since Lys⁵⁸ \rightarrow Asp side chain is shorter, it is distant from Asp⁷⁵ O δ 2.

We defined the free energies for the association reactions as following: $\Delta G_1 = \text{HLA-A2}/\beta_2\text{m}_{(\text{native})} \text{ complex} + \text{CD8}\alpha \rightarrow \text{HLA-A2}/\beta_2\text{m}_{(\text{native})}/\text{CD8}\alpha \text{ complex}$ and $\Delta G_2 = \text{HLA-A2}/\beta_2\text{m}_{(\text{Lys}\rightarrow\text{Glu})} \text{ complex} + \text{CD8}\alpha \rightarrow \text{HLA-A2}/\beta_2\text{m}_{(\text{K}\rightarrow\text{E})}/\text{CD8}\alpha \text{ complex}$. We employed free energy perturbations to calculate the relative association free energy: $\Delta G_2 - \Delta G_1 = +14.95$ Kcal/mol. These results show that the complex containing $\beta_2\text{m}_{(\text{Lys}\rightarrow\text{E})}$ has a considerable lower affinity for CD8 α than the wild type complex.

The theoretical results show that, although the contribution of the β_2 m Lys⁵⁸ to CD8 α binding is relatively small (1), its mutation should have a marked effect upon CD8 α binding.

To test these predictions, we used SPR to measure the binding of soluble CD8 α (sCD8) and soluble JM22 T cell receptor (sTCR) to HLA-A2-influenza matrix peptide complex, containing wild type or mutant β_2 m (Fig. 2). The affinity of sTCR for pMHC was similar for all of the complexes studied (Table II), indicating that the active material on the chip surface was correctly folded. However, the absolute measurements of response varied markedly between the different complexes, indicating varying proportions of active material on the chip surface. This implies that some mutant β_2 m complexes are more stable than others. In particular, HLA complexes containing Lys⁵⁸ to Tyr, Trp, SES, and GRG mutations show reduced stability (data not shown). These observations correlate with refolding efficiency, with yields of Lys⁵⁸ \rightarrow Arg and Lys⁵⁸ \rightarrow Glu complexes being several times higher than those for Lys⁵⁸ \rightarrow SES and Lys⁵⁸ \rightarrow GRG complexes (data not shown). This difference agrees with the MD simulations, which predict

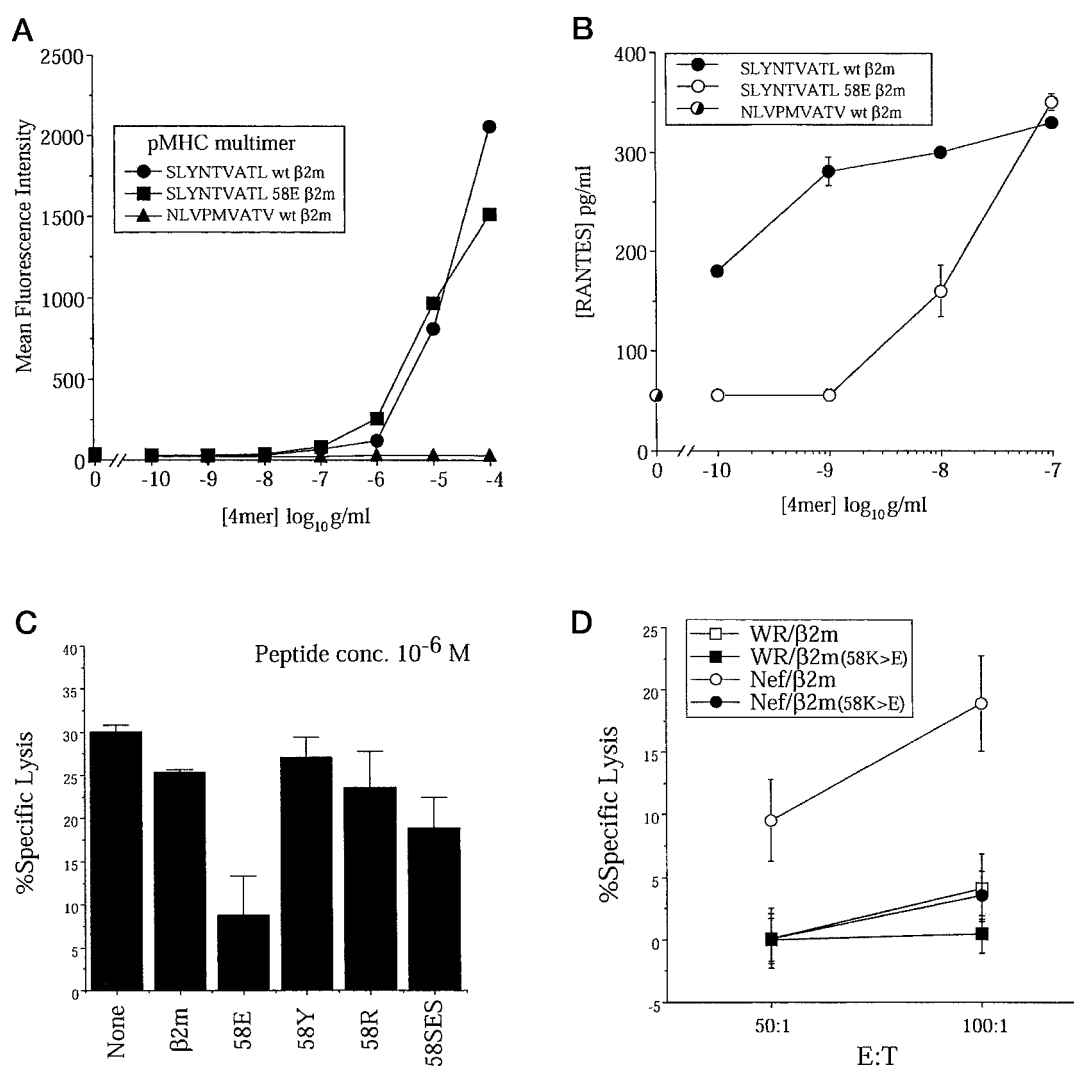


FIG. 3. Effects of soluble wild type and mutant β_2 m proteins on CD8⁺ CTL activation *in vitro*. *a*, peptide-HLA-A2 tetramers containing either wild type or Lys⁵⁸ → Glu β_2 m were folded around the HIV-1 p17-8 Gag-derived epitope SLYNTVATL (residues 77–85). Equivalent staining of the 003 CTL clone (17) at the concentrations of tetramer shown is demonstrated, consistent with previous results (2). Tetramer containing wild type β_2 m folded around the cytomegalovirus-derived HLA-A2-restricted peptide NLVPMVATV was included as a control for nonspecific binding. *b*, tetramer-induced activation of 003 CTL. Tetramers folded around SLYNTVATL containing either wild type or Lys⁵⁸ → Glu β_2 m were incubated in 96-well plates with 10⁴ CTL per well at the concentrations shown. Release of RANTES into the culture supernatant was measured after 30 min by enzyme-linked immunosorbent assay. The tetramer containing Lys⁵⁸ → Glu β_2 m induces less activation compared with the tetramer containing wildtype β_2 m at low concentrations. The control tetramer containing wild type β_2 m folded around the NLVPMVATV peptide failed to activate CTL at 10⁻⁷ g/ml. *c*, antagonism of CTL activation by soluble Lys⁵⁸ → Glu β_2 m. Target T2 hybridomas were plated at 5 × 10³ per well in 96-well round-bottomed plates with soluble proteins at 60 μ g/ml as indicated and cognate peptide at 10⁻⁶ M. After incubation for 20 min at room temperature, CTL were added at an effector:target (E:T) ratio of 2:1. Effector CTL (clone 4D5) were specific for the HLA-A2-restricted MAGE-3 tumor antigen epitope FLWGPRALV (17). The assay was harvested after 6 h. Similar results were obtained with the HLA-A2-restricted SLYNTVATL-specific CTL clone 5D8 (data not shown). *d*, inhibition of direct *ex vivo* fresh PBMC response to endogenously processed antigen. Target cells were autologous SC21 B-LCL infected with either Nef or control WR rVV as described and incubated to allow expression in the presence of 50 μ g/ml protein as indicated for 6 h. Proteins were present at this concentration throughout the ⁵¹Cr labeling process and for the entire duration of the assay. The assay was harvested after 12 h. Vaccinial expression of HLA class I-restricted antigens obviates the problems associated with potential effects of β_2 m or mutants thereof on peptide exchange at the cell surface when external loading protocols are followed. The inhibitory effect of the mutant Lys⁵⁸ → Glu protein is controlled by the addition of equimolar concentrations of wild type β_2 m. Similar results were seen in direct *ex vivo* assays with RPTYKYGAL-pulsed SC21 B-LCL (data not shown). The Lys⁵⁸ → Glu mutant also inhibited a primary CTL line (data not shown) specific for the HLA B35-restricted parvovirus B19-derived epitope QPTRVDQKM (NS1, residues 391–399) (22).

that the mutant Lys⁵⁸ → Arg complex structure is closest to that of the wild type (Table I), and that the complex containing the β_2 m Lys⁵⁸ → Glu mutant is stabilized by the interaction with HLA-A2 heavy chain R₆.

There is a strong correlation between the measured sCD8 binding (Table II) and the predicted H-bonds network formed between Lys⁵⁸ and Asp⁷⁵O δ 2 or Val²⁴O (Table I). The wild type structure forms two hydrogen bonds and shows the highest affinity for sCD8. Complexes containing β_2 m mutants Lys⁵⁸ → Arg, Ser, or Cys are predicted to form only a single H-bond (mediated through a water molecule for Lys⁵⁸ → Ser and

Lys⁵⁸ → Cys) and show decreased binding affinity for sCD8 (Fig. 2, Table II). In complexes containing other β_2 m mutants (Lys⁵⁸ mutations to Val, Asp, Tyr, Trp, GRG, SES, and Glu), where no H-bond was predicted, the sCD8 binding was negligible ($K_d > 1$ mM). Similarly, mutations of Asp⁵⁹ and Trp⁶⁰ also greatly reduced sCD8 binding (data not shown). The BIAcore binding data showed that sCD8 binding is undetectable in HLA complexes containing β_2 m in which Lys⁵⁸ is mutated to Glu (Fig. 2, Table II), yet this complex behaves identically to complexes containing wildtype β_2 m in terms of sTCR binding, refolding yield, and stability.

The strong correlation between the predictions of the molecular dynamics simulations, free energy calculations, and biophysical measurements of sCD8 binding led us to conclude that the β_2 m mutant containing a glutamate residue at position 58 (Lys⁵⁸ → Glu) was the most promising candidate for further investigation.

The impact of mutating β_2 m on the interaction between soluble antigen and TCR expressed on the cell surface was investigated using tetrameric pMHC I complexes. Fluorochrome-labeled tetramers containing either wild type or Lys⁵⁸ → Glu forms of β_2 m-stained CD8⁺ CTL at equivalent levels across a range of concentrations (Fig. 3a). However, tetrameric complexes containing the Lys⁵⁸ → Glu form of β_2 m were substantially impaired in their ability to activate CTL. This effect was titratable and most apparent at lower concentrations (Fig. 3b). These data indicate that, at similar levels of interaction with cell surface TCR, the impaired ability of complexes containing the Lys⁵⁸ → Glu form of β_2 m to engage the CD8 coreceptor translates into a biologically significant effect. This is consistent with previous work demonstrating that the major role of the CD8 coreceptor is the provision of signaling moieties that allow an enhanced sensitivity to antigen (2).

The effects of soluble exogenous wild type and mutant β_2 m proteins on CTL interactions with target cells expressing pMHC I antigenic complexes were assessed using standard ⁵¹Cr release cytolytic assays. At concentrations of pMHC on the target cell surface insufficient to saturate the maximal lytic capacity of the CTL, exogenous wild type β_2 m, and those mutants that efficiently re-fold with soluble MHC class I heavy chain to form stable complexes, consistently enhanced CTL-mediated lysis and interferon- γ production (data not shown). This effect likely relates to the ability of these proteins to stabilize pMHC class I on the target cell surface in a TCR-cognate form and is consistent with previous work (3, 20). At higher concentrations of pMHC class I on the target cell surface, exogenous mutant forms of β_2 m that impair CD8 binding to pMHC class I were found to inhibit CTL-mediated lysis (Fig. 3c). In all experiments with CD8-dependent CTL, the Lys⁵⁸ → Glu mutant was the most potent inhibitor of CTL activation. These results indicate that mutant forms of β_2 m can, through inhibition of CD8 binding to complexed pMHC I, antagonize CTL activation.

The potential use of such reagents in a therapeutic setting requires an effect on whole blood antigen-specific responses mounted by polyclonal unmanipulated CTL. We examined this using peripheral blood mononuclear cells (PBMC) isolated from donor SC21, an HIV-1-infected individual with a potent CTL response to the viral Nef protein that maps predominantly to the HLA B7-restricted epitope RPMTYK GAL (residues 75–83).

The Lys⁵⁸ → Glu mutant was found to inhibit this fresh PBMC lytic response to endogenously presented pMHC class I antigen in comparison to equimolar levels of wild type β_2 m (Fig. 3d).

In conclusion, we have developed stable β_2 m mutants that inhibit CD8 coreceptor binding to pMHC I and exert an inhibitory effect on CTL activation. These data suggest that such mutant forms of β_2 m could be used to selectively modulate the CD8⁺ cellular immune response, a principle that could be applied therapeutically (21).

REFERENCES

- Gao, G. F., Tormo, J., Gerth, U. C., Wyer, J. R., McMichael, A. J., Stuart, D. I., Bell, J. I., Jones, E. Y., and Jakobsen, B. K. (1997) *Nature* **387**, 630–634
- Purbhoo, M. A., Boulter, J. M., Price, D. A., Vuidepot, A.-L., Hourigan, C. S., Dunbar, P. R., Olson, K., Dawson, S. J., Phillips, R. E., Jakobsen, B. K., Bell, J. I., and Sewell, A. K. (2001) *J. Biol. Chem.* **276**, 32786–32792
- Rock, K. L., Rothstein, L. E., Gamble, S. R., and Benacerraf, B. (1990) *Proc. Natl. Acad. Sci. U. S. A.* **87**, 7517–7521
- Berman, H. M., Westbrook, J., Feng, Z., Gilliland, G., Bhat, T. N., Weissig, H., Shindyalov, I. N., and Bourne, P. E. (2000) *Nucleic Acids Res.* **28**, 235–242
- Brooks, B. R., Bruccoleri, R. E., Olafson, B. D., States, D. J., Swaminathan, S., and Karplus, M. (1983) *J. Comp. Chem.* **4**, 187–217
- MacKerell, A. D., Bashford, D., Bellott, M., Dunbrack, R. L., Evanseck, J. D., Field, M. J., Fischer, S., Gao, J., Guo, H., Ha, S., Joseph-McCarthy, D., Kuchnir, L., Kuczera, K., Lau, F. T. K., Mattos, C., Michnick, S., Ngo, T., Nguyen, D. T., Prodhom, B., Reiher, W. E., Roux, B., Schlenkerich, M., Smith, J. C., Stote, R., Straub, J., Watanabe, M., Wiorkiewicz-Kuczera, J., Yin, D., and Karplus, M. (1998) *J. Phys. Chem. B* **102**, 3586–3616
- Brooks, C. L., III, and Karplus, M. (1989) *J. Mol. Biol.* **208**, 159–181
- Brunger, A. T., Huber, R., and Karplus, M. (1987) *Biochemistry* **26**, 5153–5162
- Kollman, P. (1993) *Chem. Rev.* **93**, 2395–2417
- Moss, P. A., Moots, R. J., Rosenberg, W. M., Rowland-Jones, S. J., Bodmer, H. C., McMichael, A. J., and Bell, J. I. (1991) *Proc. Natl. Acad. Sci. U. S. A.* **20**, 8987–8990
- Lehner, P. J., Wang, E. C., Moss, P. A., Williams, S., Platt, K., Friedman, S. M., Bell, J. I., and Borysiewicz, L. K. (1995) *J. Exp. Med.* **181**, 79–91
- Willcox, B. E., Gao, G. F., Wyer, J. R., O'Callaghan, C. A., Boulter, J. M., Jones, E. Y., Van der Merwe, P. A., Bell, J. I., and Jakobsen, B. K. (1999) *Protein Sci.* **8**, 2418–2423
- Garboczi, D. N., Hung, D. T., and Wiley, D. C. (1992) *Proc. Natl. Acad. Sci. U. S. A.* **89**, 3429–3433
- O'Callaghan, C. A., Byford, M. F., Wyer, J. R., Willcox, B. E., Jakobsen, B. K., McMichael, A. J., and Bell, J. I. (1999) *Anal. Biochem.* **266**, 9–15
- Dunbar, P. R., Chen, J. L., Chao, D., Rust, N., Teisserenc, H., Ogg, G. S., Romero, P., Weynants, P., and Cerundolo, V. (1999) *J. Immunol.* **162**, 6959–6962
- Broder, C. C., and Earl, P. L. (1999) *Mol. Biotechnol.* **13**, 223–245
- Sewell, A. K., Gerth, U. C., Price, D. A., Purbhoo, M. A., Boulter, J. M., Gao, G. F., Bell, J. I., Phillips, R. E., and Jakobsen, B. K. (1999) *Nat. Med.* **5**, 399–404
- Price, D. A., Sewell, A. K., Dong, T., Tan, R., Goulder, P. J. R., Rowland-Jones, S. L., and Phillips, R. E. (1998) *Curr. Biol.* **8**, 355–358
- Whelan, J. A., Dunbar, P. R., Price, D. A., Purbhoo, M. A., Lechner, F., Ogg, G. S., Griffiths, G., Phillips, R. E., Cerundolo, V., and Sewell, A. K. (1999) *J. Immunol.* **163**, 4342–4348
- Shields, M. J., Kubota, R., Hodgson, W., Jacobson, S., Biddison, W. E., and Ribaldo, R. K. (1998) *J. Biol. Chem.* **273**, 28010–28018
- Xu, X., Purbhoo, M. A., Chen, N., Mongkolsapaya, J., Cox, J. H., Meier, U. C., Tafuro, S., Dunbar, P. R., Sewell, A. K., Hourigan, C. S., Appay, V., Cerundolo, V., Burrows, S. R., McMichael, A. J., and Screaton, G. R. (2001) *Immunity* **14**, 591–602
- Tolfvenstam, T., Oxenius, A., Price, D. A., Shacklett, B. L., Spiegel, H. M. L., Hedman, K., Norbeck, O., Levi, M., Olsen, K., Kantzanou, M., Nixon, D. F., Broliden, K., and Klenerman, P. (2001) *J. Virol.* **75**, 540–543